COMMUNICATION

Check for updates

Bicomponent supramolecular hydrogels derived from a Ga-based metal–organic cube and carbon-based nanomaterials

Dipayan Mandal,[a] Tarak Nath Das[b] and Tapas Kumar Maji [ID] *[ab]

1D carbon nanotubes (CNTs) and 2D graphene oxide (GO) are key components for constructing robust and versatile functional nanocomposites. Herein, we report the formation of two supramolecular hydrogels from **Ga-MOC** with GO and CNTs, facilitated by charge-assisted hydrogen-bonding interactions. Furthermore, the distinct CO_2 capture properties of these self-assembled hybrid nanocomposites are highlighted.

Composite systems are a class of materials composed of two or more distinct components, coupled through covalent or noncovalent interactions, that often exhibit unique physicochemical properties not observed in their individual constituents.[1] The ordered assembly of these nanostructures is crucial for achieving hierarchical organization and to realize their improved properties.[2,3] Incorporating low-dimensional (1D carbon nanotubes (CNTs) or 2D graphene oxide (GO)) functionalized carbon materials into this field is paramount, as they have emerged as promising candidates for a wide range of applications, including electrode materials of batteries, supercapacitors, catalysis, and recyclable absorbers.[4–9] On the other hand, hydrogels are fascinating water-insoluble, stable polymer networks with a high capacity to absorb water and biological fluids. They find widespread applications in tissue engineering, drug delivery, optics, and biomedical imaging.[10–13] When carbon-based nanomaterials such as CNTs or GO are employed as templates for introducing other molecular building blocks, they enable hybrid systems where the complementary features of two components act cooperatively to deliver superior performance in advanced applications.[14,15] Covalent polymers have been widely employed for hydrogel formation, facilitating the incorporation of CNTs or GO and offering numerous advantages for diverse applications.[15,16] So, in this study, we propose the use of a small molecular entity alongside CNTs or GO to construct hydrogels with enhanced dispersion and functionality. Here, a metal–organic polyhedron (MOP)-based hybrid system offers a promising strategy for integrating heterogeneous components such as CNTs or GO within a hydrogel matrix. Using charge-assisted hydrogen bonding (CAHB) interactions, we have designed a strategy to construct hydrogels incorporating two important carbon-based materials: amino-functionalized carbon nanotubes ($CNT-NH_2$) and GO functionalized with carboxy, hydroxy and epoxy groups (Scheme 1). The Ga^{III}-based metal organic cube (**Ga-MOC**) plays a crucial role in stabilizing these heterogeneous systems through H-bonded networks facilitating the gelation process. The resulting hydrogels were systematically investigated through various spectroscopic and microscopic methods to elucidate their structural, mechanical, and CO_2 capture properties.

The Ga^{III}-based metal–organic compound $(Me_2NH_2)_{12}[Ga_8(ImDC)_{12}]\cdot DMF\cdot 29H_2O$ was synthesized by following our previously reported procedure (Fig. S1).[17] This compound consists of two distinct components: a charged anionic cluster $[Ga_8(ImDC)_{12}]^{12-}$ (referred to as **Ga-MOC**), which shows a cubic structure, and $Me_2NH_2^+$ cations that act as charge-balancing counterions. The resulting compound consists of a supramolecular 3D extended structure formed by charge-assisted hydrogen-bonding (CAHB) between **Ga-MOC** and $Me_2NH_2^+$. Importantly, **Ga-MOC** remains stable in the molecularly dissolved state in aqueous solution.[18] However, the MOC shows a strong tendency to self-assemble *via* hydrogen-bonding interactions between its surface carboxylate oxygen and H-bond donor functional groups such as –OH, $-NH_2$, and –COOH. At elevated concentrations, these interactions promote the formation of supramolecular hydrogels through a noncovalent network assembly process. In our earlier studies, we demonstrated the formation of supramolecular nanoarchitectures and gelation of **Ga-MOC** with various small molecules possessing hydrogen-bond donor functionalities.[17,18] In the current work, we extend this approach by employing two carbon-based nanomaterials CNTs and GO as gelation partners

[a]Molecular Materials Laboratory, Chemistry and Physics of Materials Unit, School of Advanced Materials (SAMat), Jawaharlal Nehru Centre for Advanced Scientific Research, Jakkur Post, Bangalore-560064, India. E-mail: tmaji@jncasr.ac.in

[b]New Chemistry Unit, Jawaharlal Nehru Centre for Advanced Scientific Research, Jakkur Post, Bangalore-560064, India
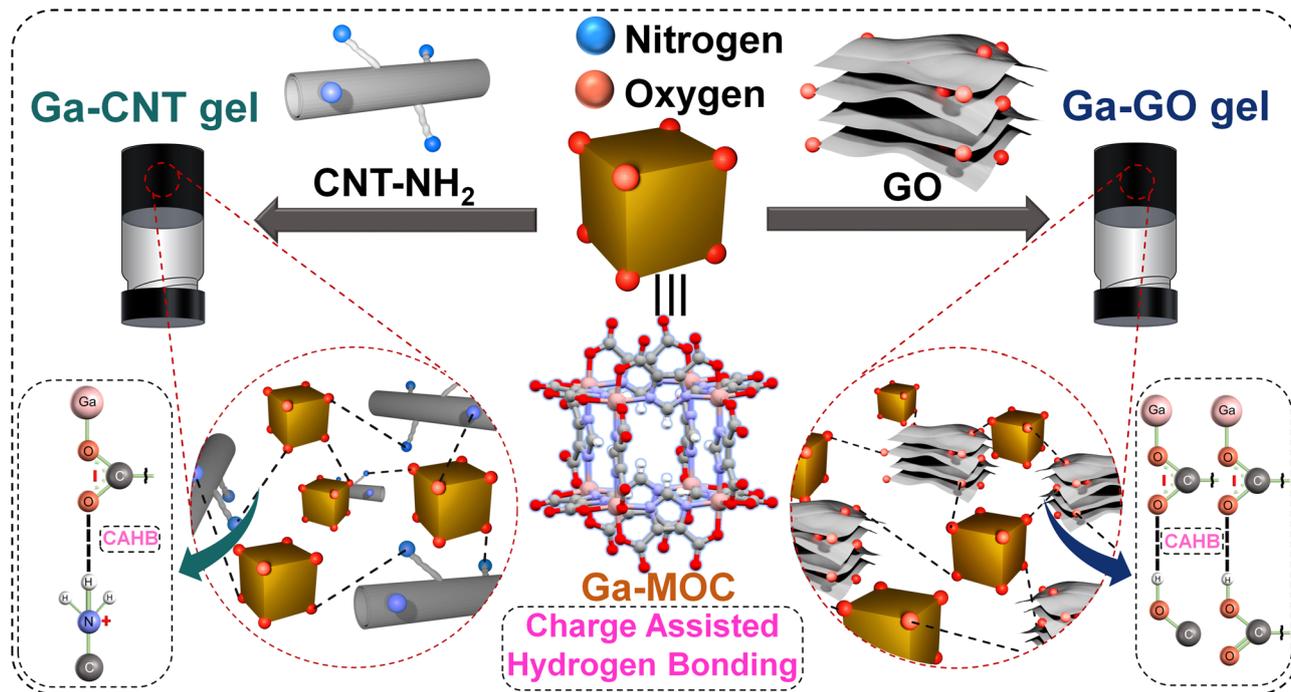
Scheme 1 Schematic representation of binder-mediated supramolecular polymerization and gel formation involving **Ga-MOC** with amino-functionalized carbon nanotubes (CNT-NH$_2$) and graphene oxide (GO).

for **Ga-MOC**. The gelation behavior of amine-functionalized multi-walled carbon nanotubes (denoted as CNT-NH$_2$) with **Ga-MOC** was first investigated. A stable dispersion was prepared by taking 3 mg of CNT-NH$_2$ in 95 μL deionized (DI) water along with 5 μL of 12 M acetic acid (AcOH) to protonate the amine groups, followed by 1 hour of sonication. The mixture was sonicated to obtain a uniform and stable dispersion, essential for effective interaction and potential gel formation with **Ga-MOC**. During the gelation experiment, **Ga-MOC** (c = 0.025 M, 100 μL) was added to the pre-dispersed CNT-NH$_2$ suspension and sonicated for a minute. However, under these conditions, no gel formation was detected, even after one week of observation. To enhance the interaction between, the amount of CNT-NH$_2$ was increased to 6 mg, while maintaining all other parameters constant. This modification resulted in the rapid formation of a stable gel within 1 hour (Fig. 1a). Gelation is likely driven by hydrogen-bonding interactions between the carboxylate groups of **Ga-MOC** and the protonated amine groups (–NH$_3^+$) on the surface of CNT-NH$_2$. The resulting gel, denoted as **Ga-CNT** gel, appeared black in color, attributed to the intrinsic colour of CNT-NH$_2$. The critical gelation concentration (CGC) of CNT-NH$_2$ was 22.5 mg mL^{-1} with 45 mg per mL **Ga-MOC**, confirmed by vial inversion and rheology study, indicating viscoelastic gel behavior. Within the linear viscoelastic region, the storage modulus (G') consistently exceeded the loss modulus (G''), and both moduli remained nearly parallel, signifying gel-like behavior (Fig. 1b).[19] The loss factor (tan δ = G''/G') at 0.1% strain was calculated to be 0.48, further supporting the formation of a stable supramolecular hydrogel. This gel exhibited shear-thinning behavior, as evidenced by its shear stress $vs.$ shear rate profile (Fig. S3a). Interestingly, no gel formation was observed in the absence of AcOH, suggesting the crucial role of protonated amine groups in strengthening the H-bonds through electrostatic interaction, thereby facilitating the gelation process. To obtain the corresponding aerogel, the **Ga-CNT** hydrogel was subjected to critical point drying (CPD) for the removal of water. Powder X-ray diffraction (PXRD) of the resulting aerogel confirmed the presence of both **Ga-MOC** and CNT-NH$_2$, as evidenced by the retention of characteristic diffraction peaks from both components (Fig. 1c). Raman spectroscopy further validated the presence of CNT-NH$_2$ through the observation of the D band ($\sim$1312 cm^{-1}) and G band ($\sim$1609 cm^{-1}) (Fig. S4a). Morphological analysis of the **Ga-CNT** aerogel was performed using field-emission scanning electron microscopy (FESEM) and transmission electron microscopy (TEM), which revealed the presence of tubular nanostructures (Fig. 1d and e). Elemental mapping analysis confirms the presence of Ga, C, N and O together, which validated the self-assembly of **Ga-MOC** with CNT-NH$_2$ (Fig. 1d). Zeta potential measurements of the **Ga-CNT** aerogel dispersion exhibited a negatively charged surface species (Fig. S5a). In contrast, CNT-NH$_2$ showed a positive zeta potential, which increased in the presence of acetic acid due to the protonation of the amine groups (Fig. S5a). Only **Ga-MOC** exhibited a distinctly negative zeta potential, which was retained in the **Ga-CNT** aerogel but with reduced magnitude due to the partially protonated CNT-NH$_2$ offsetting the charge. To further confirm the pivotal role of **Ga-MOC** in self-assembly and gelation, the CNT-NH$_2$ dispersion in water was stored for a week and remained a stable, free-flowing solution. The N$_2$ adsorption
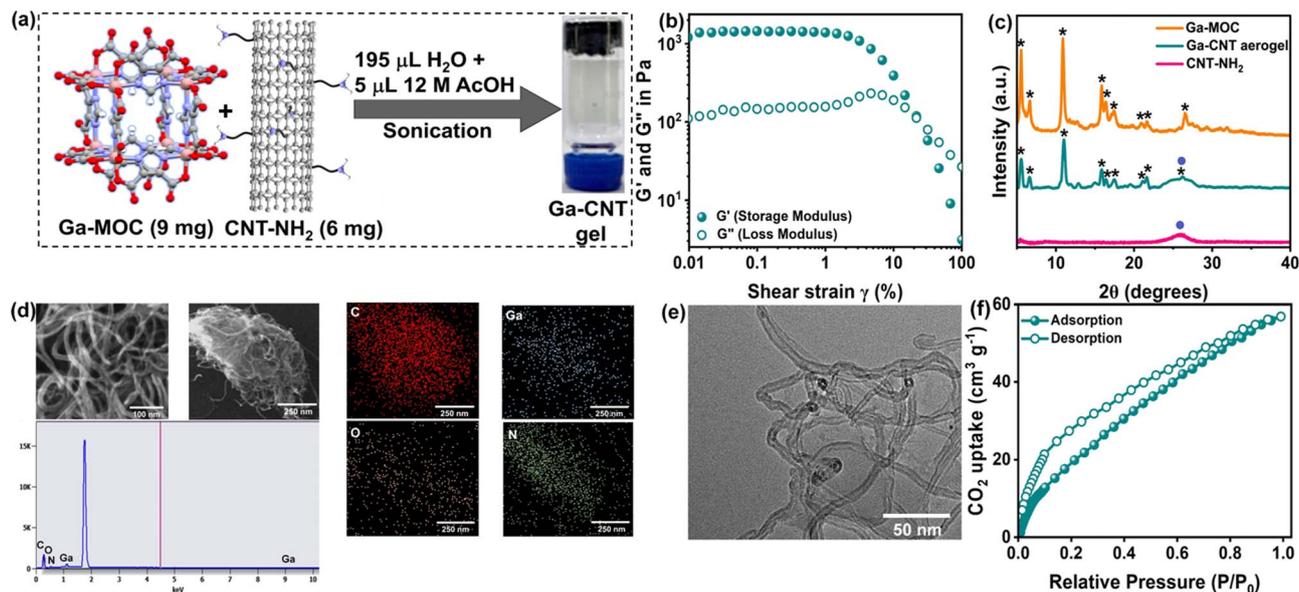
Fig. 1 (a) Schematic showing the formation of **Ga-CNT** gel. (b) Strain sweep rheology measurement of **Ga-CNT** gel. (c) PXRD patterns of CNT-NH₂, **Ga-MOC** and **Ga-CNT** aerogels. (d) FESEM and EDS of **Ga-CNT** aerogel. (e) TEM image of **Ga-CNT** aerogel. (f) CO₂ adsorption–desorption isotherm of **Ga-CNT** aerogel at 298 K.

isotherm for **Ga-CNT** aerogel measured at 77 K revealed a surface area of 61 m^2 g^{-1} (Fig. S6a).

The gelation study was further extended to GO, which contains –OH, –O–, and –COOH groups that can promote self-assembly with **Ga-MOC**. GO was synthesized from graphene using the modified Hummer's method[20] and characterized by spectroscopic and microscopic analyses. Further characterization using PXRD, Raman spectroscopy, and FESEM-EDS elemental mapping collectively confirmed the successful oxidation of the graphene nanosheets (Fig. S2). This oxidation process generates functional groups, including hydroxyl (–OH) and carboxyl (–COOH), on the graphene surface, thereby facilitating hydrogen-bond-driven assembly with **Ga-MOC**. Initially, 3 mg of GO was dispersed in 100 μL of deionized water and sonicated for 1 hour to obtain a uniform suspension. This dispersion was added to a separately prepared solution of **Ga-MOC** ($c = 0.025$ M, 100 μL). However, upon storing the mixed solution for a week, no gelation was observed, while increasing the GO amount to 6 mg under the same conditions led to successful gelation described as **Ga-GO** gel (Fig. 2a). The CGC of GO was 30 mg mL^{-1} with 45 mg per mL **Ga-MOC**, as confirmed by vial inversion and rheology study, indicating a viscoelastic hydrogel network. The viscoelastic behaviour of the **Ga-GO** gel was found to be similar to that of the CNT analogue, with the storage modulus exceeding the loss modulus in the linear viscoelastic region (Fig. 2b). Additionally, at 0.1% strain, the loss factor (tan $\delta = G''/G'$) was calculated to be 0.35, confirming successful gelation. Similar to the previous gel, the shear stress $vs.$ shear rate profile of this gel also demonstrates shear-thinning behavior (Fig. S3b). The corresponding **Ga-GO** aerogel was obtained by drying the gel with CPD. The PXRD pattern of the aerogel confirmed the coexistence of **Ga-MOC** and GO (Fig. 2c), as characteristic diffraction peaks from both

components were observed. The Raman spectrum further validated the presence of GO, with prominent D band (1322 cm^{-1}) and G band (1602 cm^{-1}) characteristic of oxidized graphene sheets (Fig. S4b). AFM, FESEM and TEM analyses revealed a 2D nanosheet-like morphology for the **Ga-GO** aerogel (Fig. 2d, e and S7), with elemental mapping confirming uniform distribution of Ga, C, N, and O (Fig. 2d). No isolated **Ga-MOC** clusters were observed, indicating uniform integration via hydrogen bonding. Zeta potential measurements showed a reduced negative charge for **Ga-GO** aerogel compared to GO, reflecting surface charge masking upon assembly (Fig. S5b). Despite negative charges on both components, gelation is driven by hydrogen bonding interaction. The **Ga-GO** aerogel showed a surface area of 80 m^2 g^{-1} (Fig. S6b) as realized from the N₂ adsorption isotherm at 77 K. Next, we conducted CO₂ uptake studies at 298 K to understand the effect of the nanocomposites based on hydrogel formation. The **Ga-CNT** aerogel showed a CO₂ uptake of 57 mL g^{-1} at $P/P_0 = 1$ (Fig. 1f), likely due to Lewis acid–base interactions between CO₂ and the –NH₂ groups, whereas the **Ga-GO** aerogel exhibited a lower uptake of 17 mL g^{-1} at $P/P_0 = 1$ (Fig. 2f). We repeated the CO₂ adsorption experiment to assess structural stability, and the results confirmed good stability (Fig. S8).

In summary, we developed two supramolecular hydrogels using CNT-NH₂ and GO, mediated by a discrete Ga-based metal–organic cube (**Ga-MOC**). The carboxylate oxygen atoms in **Ga-MOC** act as hydrogen-bonding acceptors, interacting with functional groups on the carbon-based materials to drive self-assembly. Importantly, we emphasize the unique role of CAHB interactions in hydrogel formation, where **Ga-MOC** acts as an integrated component in the self-assembly with the carbon-based materials. Comprehensive spectroscopic and microscopic analyses confirmed the formation of
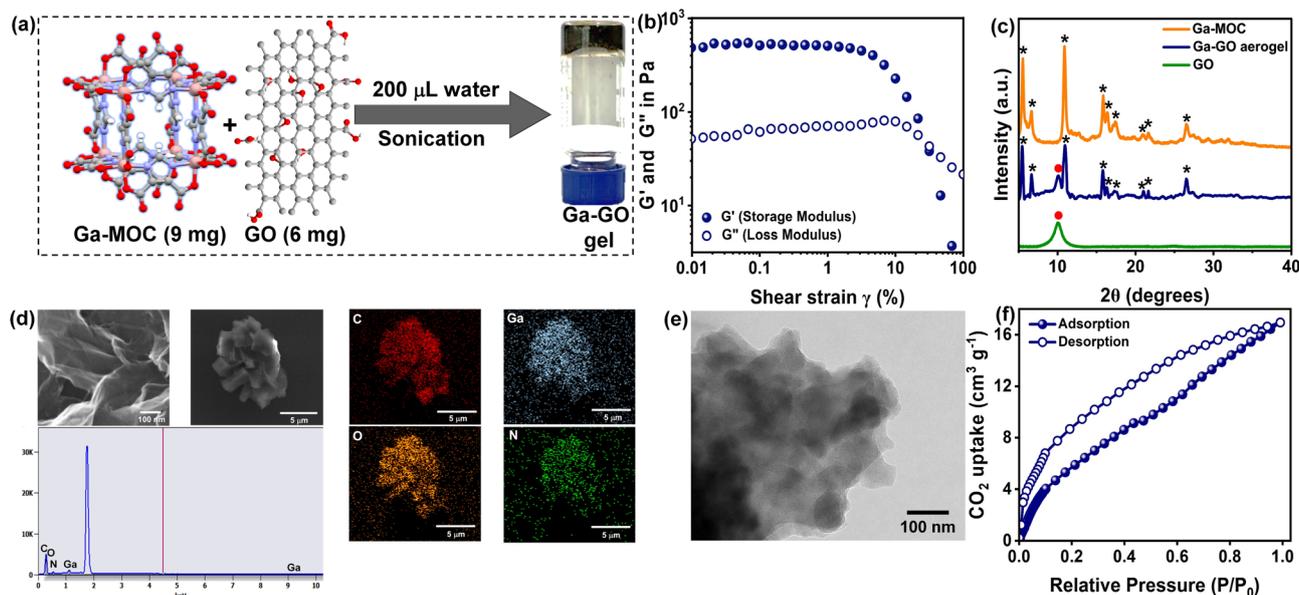
Fig. 2 (a) Schematic showing the formation of **Ga-GO** gel. (b) Strain sweep rheology measurement of **Ga-GO** gel. (c) PXRD patterns of CNT-NH₂, **Ga-MOC** and **Ga-GO** aerogels. (d) FESEM and EDS of **Ga-GO** aerogel. (e) TEM image of **Ga-GO** aerogel. (f) CO_2 adsorption–desorption isotherm of **Ga-GO** aerogel at 298 K.

nanostructures in the hybrid composite materials. The **Ga-CNT** aerogel further exhibited significant CO_2 adsorption, likely due to Lewis acid–base interactions between CO_2 molecules and –NH_2 groups. Overall, this work demonstrates that small metal–organic polyhedral units can organize heterogeneous carbon-based materials while preserving their structure, offering a simpler and more efficient alternative to polymer-based methods.

Author contributions

D. M. and T. K. M. designed the concept of this work. D. M. performed all the major experiments. D. M., T. N. D., and T. K. M. analysed all the experimental data. D. M., T. N. D., and T. K. M. wrote the manuscript. All authors discussed the results and commented on the manuscript.

Conflicts of interest

There are no conflicts to declare.

Data availability

The data supporting this article have been included as part of the supplementary information (SI). Supplementary information is available. See DOI: **https://doi.org/10.1039/d5na00869g**.

Acknowledgements

Notes and references

1 A. S. Thomas, P. N. Immanuel, N. Prasad, A. Goldreich, J. Prilusky, R. Carmieli and L. Yadgarov, *Nanoscale Adv.*, 2025, **10**, 1039.

2 W. Eom, E. Lee, S. H. Lee, T. H. Sung, A. J. Clancy, W. J. Lee and T. H. Han, *Nat. Commun.*, 2021, **12**, 396.

3 F. Schütt, S. Signetti, H. Krüger, S. Röder, D. Smazna, S. Kaps, S. N. Gorb, Y. K. Mishra, N. M. Pugno and R. Adelung, *Nat. Commun.*, 2017, **8**, 1215.

4 I. A. Kinloch, J. Suhr, J. Lou, R. J. Young and P. M. Ajayan, *Science*, 2018, **362**, 547–553.

5 J. Kim, L. J. Cote and J. Huang, *Acc. Chem. Res.*, 2012, **45**, 1356–1364.

6 A. S. Aricò, P. Bruce, B. Scrosati, J.-M. Tarascon and W. Van Schalkwijk, *Nat. Mater.*, 2005, **4**, 366–377.

7 L. L. Zhang and X. S. Zhao, *Chem. Soc. Rev.*, 2009, **38**, 2520.

8 Z. Zhang, T. Sun, C. Chen, F. Xiao, Z. Gong and S. Wang, *ACS Appl. Mater. Interfaces*, 2014, **6**, 21035–21040.

9 H. Sun, Z. Xu and C. Gao, *Adv. Mater.*, 2013, **25**, 2554–2560.

10 K. Y. Lee and D. J. Mooney, *Chem. Rev.*, 2001, **101**, 1869–1880.

11 R. Narayanaswamy and V. P. Torchilin, *Molecules*, 2019, **24**, 603.

12 Md. S. B. Sadeque, H. K. Chowdhury, M. Rafique, M. A. Durmuş, Md. K. Ahmed, Md. M. Hasan, A. Erbaş, İ. Sarpkaya, F. Inci and M. Ordu, *J. Mater. Chem. C*, 2023, **11**, 9383–9424.

13 Y. C. Dong, M. Bouché, S. Uman, J. A. Burdick and D. P. Cormode, *ACS Biomater. Sci. Eng.*, 2021, **7**, 4027–4047.

14 S. H. Kang, G. Y. Lee, J. Lim and S. O. Kim, *ACS Omega*, 2021, **6**, 19578–19585.

15 H. Lu, S. Zhang, L. Guo and W. Li, *RSC Adv.*, 2017, **7**, 51008–51020.

16 Y. Zhu, D. K. James and J. M. Tou, *Adv. Mater.*, 2012, **24**, 4924–4955.

17 P. Sutar, V. M. Suresh, K. Jayaramulu, A. Hazra and T. K. Maji, *Nat. Commun.*, 2018, **9**, 3587.

18 T. Nath Das, R. Jena, G. Ghosh, G. Fernández and T. K. Maji, *Angew. Chem., Int. Ed.*, 2025, **64**, e202421536.

19 S. Mondal, F. A. Rahimi, T. N. Das, S. Nath and T. K. Maji, *Chem. Sci.*, 2025, **16**, 3646–3654.

20 X. Chen, Z. Qu, Z. Liu and G. Ren, *ACS Omega*, 2022, **7**, 23503–23510.